Development of treated cardboard waste injection machine into the sandy soils

Ahmed Shawky El-Sayed,[1] Ibrahim Said Mosaad[2]

[1]Department of Agricultural Bioengineering Systems, Agricultural Engineering Research Institute, Agricultural Research Centre, Giza, Egypt; [2]Department of Soil Fertility and Plant Nutrition, Soil, Water and Environment Research Institute, Agricultural Research Centre, Giza, Egypt

Abstract

This study aimed to evaluate a new prototype for an injection machine that works in sandy soils using treated cardboard waste. The tests were divided into three major categories: i) the first one was a performance evaluation of the new injection prototype; ii) secondly, study the effect of adding the treated cardboard to the sandy subsoil on reducing the irrigation levels and increasing the moisture content in the root zone of cultivated plants; and investigate sandy soil water storage efficiency and its impact on improving the soil's properties; thirdly, measurements on water-sensitive crop yields, like potatoes. The new prototype technique was designed using an integrated automatic control system to precisely control the injection discharge rate. So, the injection operation is proportionally synchronised with the tractor's forward speed. The field experiments were carried out at 0.24, 0.40, 0.57, and 0.74 m sec^{-1} of tractor forward speeds with 250, 350, and 450 mm of furrow openers' subsoil depths at 140 and 200 mm of injection widths and 5 and 10% concentrations of cardboard solution. The main results indicated that the maximal consumed energy was 196.08 kWh ha^{-1} with a field efficiency of 89.05% and an optimal field capacity of 0.281 ha h^{-1} using the highest variable levels. In addition, the water-saving percentage was 35.80%, while the water storage efficiency was 85.85%. Furthermore, the total economic costs were reduced by 13.88% compared to the traditional silt injection method for the tested control plots.

Correspondence: Ahmed Shawky El-Sayed, Department of Agricultural Bioengineering Systems, Agricultural Engineering Research Institute, Agricultural Research Centre, Giza, Egypt.
E-mail: a.shawky71@yahoo.com

Key words: Concentrations; discharge; furrow openers; prototype; specific draft; water storage.

Acknowledgements: this work was supported by the Agricultural Engineering Research Institute (*AEnRI*) and the Soil, Water, and Environment Research Institute (*SWERI*), Agricultural Research Centre (*ARC*), Egypt, by providing the laboratory equipment and raw materials which were used to manufacture this injection prototype.

See the online Appendix for additional Figures and Tables.

Received for publication: 18 January 2022.
Accepted for publication: 12 July 2022.

*Journal of Agricultural Engineering 2022; LIII:1354
doi:10.4081/jae.2022.1354*

Introduction

Sandy soils offer advantages and disadvantages when compared to clay soils. They require more water, fertiliser, and amendments, but they are easier to work with, and many plants prefer this type of soil (Uzoma *et al.,*2011). Sandy soils contain large soil particles, which means there are large pores between the particles. These large pore spaces allow water to drain quickly and easily through the soil. Because of this simple fact, sandy soil drains quickly and does not contain much water. The inability of sandy soils to retain water is considered one of the most substantial challenges of the agricultural expansion in the desert lands spread over a large scale worldwide. Water availability and the soil's ability to hold water for as long as feasible are key factors in agriculture. The waste of cardboard, which is assessed as a global environmental problem, may be an effective and economical solution to the sandy soil's inability to hold water. Saving water resources on agricultural soils is a key goal of the global water strategy to serve the census's growing population. As a result, bio-system integrated methods must be used to solve this partial problem. Obviously, sandy soils are defined as soils with an average sand content of greater than 50% percent and less than 20% clay content at 300 mm depth (Hengl *et al*., 2017). Thus, most sandy soils suffer from bad physical features such as their weak structure, poor water retention, higher permeability, and highly sensitive compaction with several adverse consequences (Bechtold and Naiman, 2006; Tutwiler, 2021). In fact, the infiltration rate in sandy soils is likely to be about 250 times lower than in clay soils (Balba, 1995). The physical properties of sandy soils, like bulk density and porosity, aggregate vary largely because of the size and organization of the grains, clay type, and agricultural operating activities such as tillage (Bruand *et al*., 2004). Significant spatial and temporal variations in evapotranspiration and deep added retained materials drainage were due to the related uniformity of sandy soil particle size distribution (Paço *et al*., 2006; Alberto *et al*., 2011; Nocco *et al*., 2019). Likewise, the improvement process for sandy soils is considered among the most economical engineering solutions to overcome their watering problems.

However, the significance of these techniques has grown, particularly when industrial waste is mixed with soil (ElMashad and Hashad, 2013). As well, Rao *et al.* (2012) showed that sandy soils were improved by admixture stabilisation and fibre reinforcement, which represented an effective mixing method. Increasing the subsoil organic materials improves its properties due to its developing structure. Using this matter reduces the soil infiltration rates and increases water retention through the root zone of growing plants. According to studies by Huntington (2006), the porosity decreased in the root depth zone, reserving the plant's available moisture content at a high percentage. When bulk density increases, it invariably results in relatively high penetration resistance with significant root vegetative growth (Bengough and Mullins, 1991). Besides, the active root zone had the potential to return water moisture from the atmosphere via evapotranspiration and the zone depth, which affected the exchange between water vapor and soil moisture with the observing levels with a positive significant effect (Guswa, 2008). The farmer could determine the irrigation accurately from the periods of irrigation and the in-between time due to estimating the soil water storage capacity (Nyvall, 2002). Generally, water use efficiency is achieved through many improvement methods by increasing water delivery methods and application time through irrigation. The irrigation methodology was directly related to the mechanism of plant drought tolerance (Sezen *et al.,* 2011). Furthermore, industrial cardboard is made of recycled fibre pulp, which has physical water-preservation properties. Moreover, supplementing the cardboard waste in the subsoil may have the advantage of retaining the soil moisture content for an extended period. Also, cardboard was classified as residue with less nutrient levels and the maximum C/N ratio, thus promoting decrement ratios for the microorganisms' decomposition speed. As a result, it improved its retention in sandy soils for in-between irrigation periods, resulting in an improvement in sandy soil properties from its water retention ability to the longest possible period, which reduced irrigation rates during planting seasons (Mazza *et al*., 2014). The potato was selected for experiments, and it is a strategic crop that grows well in sandy soil and is one of the crops that consumes irrigation water. Clearly, the irrigation of sensitive water-stressed crops like potatoes requires a systematic approach to irrigation scheduling (Ayas, 2013). However, drip irrigation gained significant increment ratios in the growth parameters levels, the yield of potato tubers, in particular, owing to increased irrigation level (Badr *et al.*, 2012). Various research studies have studied the addition of some materials, whether chemical additives or agricultural waste, to improve the characteristics of sandy land to reduce water use. However, Ling *et al.* (2021) stated that using biochar improved the sandy soils' water retention, the water holding capacity, and the crop's resistance to drought, but it needed more production costs. Also, Algadwi *et al.* (2021) showed a positive effect on all types of soils when experimentally using polymer additives, except in the sandy soils kind, where the level of contamination was very low. Also, Malerba and Cerana (2020) stated the effect of using chitin-and chitosan-based derivatives in plant protection against biotic and abiotic stresses in sandy soils. As well, Asamatdinov (2018) stated that the effect of using polymer additives in sandy soils had a significant effect on reducing water use. Also, Fuat *et al.* (2018) stated that adding layers of grass, cardboard, and sawdust to water holding capacity was studied, which reduced soil erosion rates and increased water absorption rates while reducing nitrogen fertilization rates and increasing plant productivity in sandy soil. Also (Adugna, 2016) stated the effect of using compost on improving soil properties and maximising crop productivity in such sandy soils. Also, El-Halim and Kumlung (2015) studied the effect of adding bagasse additive to the sandy soils only in the laboratory to improve the hydro-physical features. Sandy soils need to be improved, whether artificial or natural, which is considered an additional economic cost. Clay soil and silt transported to reduce water permeability in the root zone contain some alkaline substances or weed seeds, which reduce productivity (Duncan *et al*., 2000). Therefore, cardboard waste was used, which is a safe alternative because it is free from any chemical effect on the nature of the soil as it consists mainly of cellulose fibres, which can save water without affecting the rate of root spread. In addition to the low price of this waste and its large quantities, it can be treated in easily, unlike other additives. In practice, the addition of a layer of cardboard in the root zone has proven to have a significant positive effect on reducing irrigation rates (Fuat *et al.,* 2018).

This study aimed to investigate the mechanical and economic performance of a new cardboard injection prototype that uses treated cardboard residues to improve the physical properties of sandy soils. Also, it studies the effect of using cardboard waste on preserving soil moisture content, saving water for longer durations in the plant root zone, and on decreasing irrigation rates.

Materials and methods

Study area

The field experiments were carried out during two following growing seasons (2020-2021) from February to June for the potato crop. The field experiments were conducted in the Qalabsho farm, El_Dakahlia governorate, Egypt (latitude 25′ 31°-30′ 31° N, and longitude 27′ 31°-18′ 31° E). The experimental design was set up in a four-way, completely randomised design to investigate the tested variables. The first factor (*S*) included four forward speed levels (0.24, 0.40, 0.57, and 0.74 m sec-1) changed using a tractor transmission system. The second factor (*D*) included three subsoil injection depths of (250, 350, and 450 mm) which were changed using mechanical sliders. The third factor (*W*) included two injection cardboard operation widths of (140 and 200 mm) changed by using three or five distribution nozzles, respectively. Besides the fourth factor (*C*) included two cardboard solution concentrations of (5 and 10%) changed by the added water to the mixed cardboard (50 g: 1L) and (100 g: 1L), respectively. The experiments were done using four replicates (192 plots). Every plot equals 30 m^2 (total area: 0.576 ha) (5 rows, 10 m long and 0.6 m wide). Seed tubers of the cultivar *Spunta* were planted with a space of 0.25 m between plants. Drip irrigation was applied according to standard recommendations and stopped a week before harvest. The fertilisation and pest control programs were implemented according to the recommendations of the Egyptian Ministry of Agriculture. The soil properties of the experimental site were analysed as listed in Appendix Table 1.

Design of the cardboard waste injection machine

The new design of the injection prototype was fabricated to suit the sandy zones within multi-mechanical control options, such as controlling the subsoil injection depth and width to fit various crops. The prototype performs multiple operations, including cutting cardboard and mixing it with water to create a semi-liquid paste. Cardboard waste free from colours, glues, and some metals was used. The cardboard residues used in the injection process were from food manufacturing waste, such as those used in the packaging of table eggs. The chemical analysis of the used cardboard waste was carried out in the laboratory, which contained cellulose of 82%, hemicellulose of 16.5%, and lignin of 1.5%, respectively, while the cardboard sheet thickness was 5 mm. The reused cardboard features are suitable for organic farming as there are no pollutants in them, and they positively affect soil properties in terms of moisture retention. A new design of furrow openers was explicitly manufactured for sandy soils to perform injection operations. The injection operations were precisely done by using an automatic control system for the cardboard injection valves and a digital control timer that controlled the distributor nozzles attached to the furrow openers, as shown in Figures 1 and 2. The innovative injection prototype specifications are detailed in Appendix Table 2.

As shown in the schematic drawing (Figure 1), the cardboard injection prototype dimensions from the total length, width, height, and operating width were mentioned. The prototype chassis was mounted on the tractor using the three-hitching point system. The chassis was designed and formed with the method of reassembling to facilitate its storage and control of the operational width and depth. Also, the chassis was designed to withstand various compression and tension loads while maintaining a suitable safety factor. The subsoil penetration units (digger-type furrow openers), as shown in (Figure 1, no.1) were designed according to the calculations of different engineering stresses to suit tough operational conditions in the new sandy reclaimed soils. The furrow openers were classified as a digger type and had approximate dimensions of 400×300×250 mm in length, width, and height. The actual operation width equals 300 mm from the bottom of the subsoil slash. In addition, the furrow openers were combined with the chassis *via* two types of sliders: the longitudinal slider, which is used to set the injection operation depth, and the transverse slider, which is used to set the injection operation depth as shown in (Figure 1, no.4). The cardboard injector units consisted of two distributors, which were made from polyethylene pipes (25.4 mm diameter and 300 mm length) and were shuttered laterally. Each distributor is supplied with five straight copper nozzles (10 mm in diameter and 50 mm in length) (Figure 2A and B). Every distributor was connected to a flexible discharge hose (25.4 mm diameter) that was connected to the cardboard mixing unit, as shown in (Figure 1, no.2). In addition, the prototype included a soil covering unit, as shown in (Figure 1, no.3), that was used to cover the engraved soil slashes and was fixed on the rear side behind the furrow opening lines. This covering unit was connected to the chassis frame with a lateral slider (Figure 3, no.5) to be used at the needed injection depth for the planted crop.

Furthermore, the mixing unit, which is in charge of shredding and mixing the treated cardboard, is comprised of an electrical mixer supplied with an alternating current motor, the specifications of which are listed in Table 3. The driving motor was attached to the reduction gearbox by a V belt (1625×13 mm) to mix and pre-

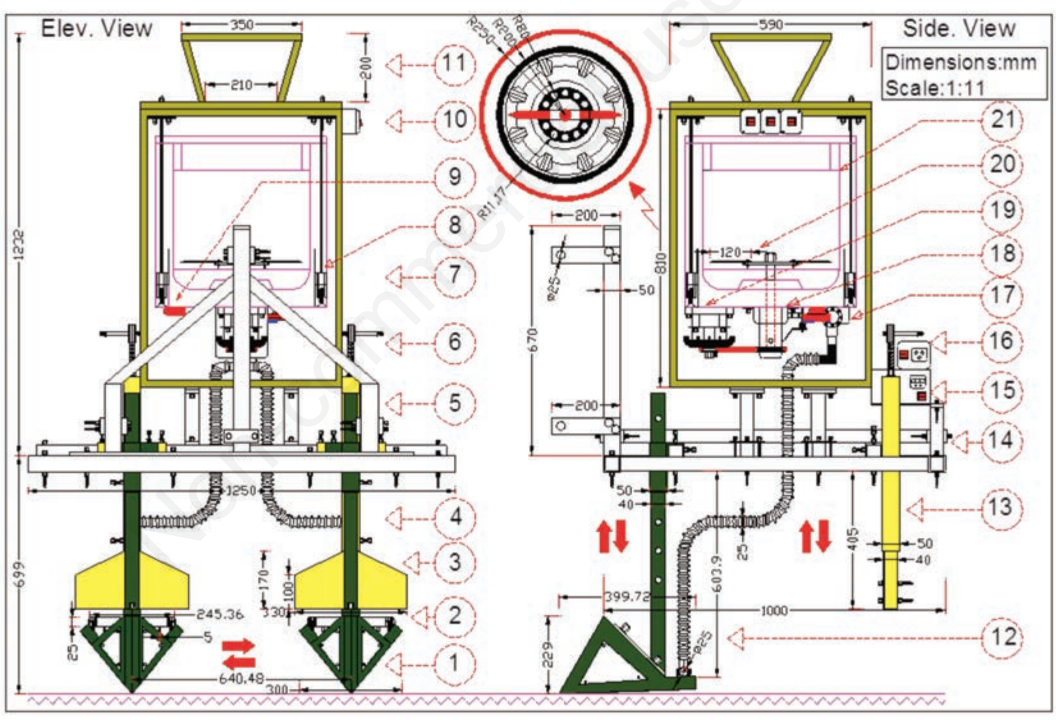

1	Furrow opener	8	Shock absorber	15	Digital controller unit
2	Distribution nozzles	9	Stirring motor capacitor	16	DC-AC inverter 1500W
3	Sweeping coverage unit	10	Right and left side rotation and tensioner motor electrical switches	17	Discharge valve
4	Furrow opener longitudinal slider	11	Feeding hopper	18	Gearbox
5	Three hitching point	12	Discharge hose	19	Stirring AC motor
6	Covering unit tensioner	13	Coverage crane	20	Cutter blades
7	Mixing unit outer body	14	Idler tensioner	21	Inner stainless-steel cistern
DC	Direct current, 12V	AC	Alternating current, 220V		

Figure 1. The cardboard injection prototype schematic drawing (dimensions: mm).

pare the injected liquefied dough cardboard into the sandy subsoil, as shown in (Figure 4B, no.2). As shown in Figure 3, no.7, the mixing unit was controlled electronically using direct operating press switches. The used gearbox had a reduced rotation speed ratio of (1:4) from 600 to 150 rpm for the cardboard cutting blades. Furthermore, the gearbox included an electrically controlled mechanical transmission system that was used to increase the rotation speed of the motor at a 1:1 ratio *via* a lever that was electrically attracted by an electrical tensioner motor (Figure 4B, no.3).

The electrical control circuit is shown in Figure 5A was designed to facilitate operating operations automatically by the tractor operator using connecting switches. The primary source of the electrical power that was used in the prototype was connected from the tractor's battery (12V-150 A) to an alternative current inverter (1500 W) of the modified wave type (Figure 5B, no.1) to feed the prototype electronic circuit. Then the electrical power was connected to the driving bi-directional motor (220V-205 W) (Figure 4B, no.1) to rotate the cutter blades of the cardboard mixer (Figure 3A). There are two operational systems: the first is a fully automatic system that uses a twin digital timer (Figure 5B, no.2) to control the timing of the electrical tensioner motor to automatically control the outlet cardboard mechanical valve (Figure 4B, no.5). Second: the manual operating system included three direct switches, to connect directly to the mixer unit from both rotation sides and open the cardboard injection pass directly, as shown in (Figure 1, no.10). Where the automated system is used in the field when operating, while the manual system is used when preparing and calibrating the cardboard before performing the injection process. As shown in (Figure 5A), a small flashing buzzer was used to alert the user that the injection operation was underway. The used cardboard waste was classified by thickness, ranging from 410 to 610 µm (Twede *et al.,* 2014).

Mechanical performance of the injection prototype

First, the mechanical performance of the injection prototype was estimated by measuring the injection rate (*Ir*) and thickness (*Lt*), as shown in Eq. 1 and Appendix Table 4.

$$Ir= \frac{dr\times 4200\times 2.4}{1000} \quad (1)$$

where: *Ir*: injection rate, m^{3}ha^{-1}; *dr*: discharge rate, L m^{-2}; 4200: constant; 1000: constant; *dr*: the discharge rate, L sec^{-1}.

Also, the fuel consumption (*F*) was determined using the topping-off method according to Manzone (2015). The prototype-specific energy consumption (*CE*) was estimated according to Hunt, 1983 as presented in the Eq. 2 and 3. Finally, the prototype field efficiency (*Fe*) and field capacity (*FC*) were determined according to the methodology of Kepner *et al*. (1982).

$$CE = \left(\frac{Fs\times\rho_f\times C.V}{3600}\right)\times\left(\frac{427\times\eta_{th}\times\eta_m}{75\times 1.36\times FC}\right)+EP \quad (2)$$

$$Ep=I*V*\eta*\cos\varphi/1000 \quad (3)$$

where: *CE*: prototype consumed energy, (kWh ha^{-1}); *Fs*: fuel consumption rate, (L h^{-1}); ρ_f: density of fuel, kg L^{-1}, (for diesel=0.85 kg L^{-1}); *C.V* : the calorific value of fuel, (kcal kg^{-1}); 427: thermal-mechanical equivalent, (kgm kcal^{-1}); η_{th}: thermal efficiency of the engine, assumed 40% for the diesel engine; η_m: mechanical efficiency of the engine, assumed 80% for a diesel engine; *Fc*: actual field capacity, ha h^{-1}; *EP*=electrical consumed power under different machine loads; *I*=line current strength in Amperes; *V*=potential difference (voltage) is equal to 220 *V*; $h_{m=}$mechanical efficiency (assumed as 80%); *cos* φ=power factor (was taken as 0.7).

Besides determining the draft force (*dF*) and the specific draft (*Sd*) by using the tractor drawbar pull method and a dynamometer as presented in Eq. 4, according to (Smith *et al.*, 1994). Furthermore, using the (Oida, 1997) methodology to estimate the total operating cost (*TC*) for the injection prototype, as shown in Eqs. 5-7.

$$Sd=dF\times 1000/A \quad (4)$$

where: *Sd*: specific draft, Pa; *dF*: draft force; kN; *A*: area, m^2.

$$C=\frac{P}{h}\left[\frac{1}{a}+\frac{I}{2}+T+r\right]+(W.e)+\frac{m}{144} \quad (5)$$

$$OC=\frac{Machine\ \text{hourly cost}}{Actual\ \text{field}capacity} \quad (6)$$

$$TC= OC + IC \quad (7)$$

where: *C*: hourly machine cost, USD h^{-1}; *OC*: operating cost, USD

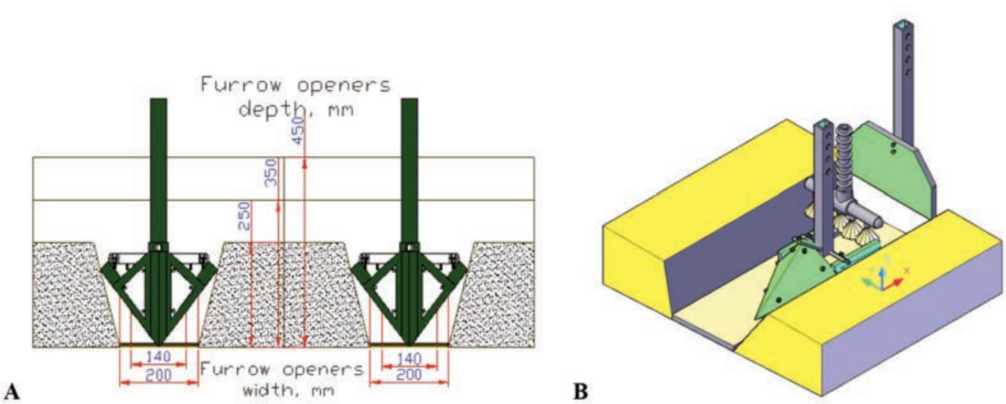

Figure 2. The soil cross section using the furrow openers: A) 2D drawing; B) isometric (dimensions: mm).

h^{-1}; *TC*: total cost, USD h^{-1}; *IC*: injection material cost, USD.h^{-1}; *P*: machine price, USD; *h*: yearly working hours, h year^{-1}; *a*: machine life expectancy, year; *I*: annual interest rate; *T*: tax overheads ratio; *r*: repair and maintenance ratio; *W*: motor power, kW; *e*: hourly cost per kW.h.; *m*: monthly average wage, USD; and 144: monthly average working hours.

The operating cost (*OC*) of the equipment and the tractor was calculated, including the cost of fuel consumption and maintenance. In addition, the quantity of the injected substance was calculated per cubic meter, which differed according to the different treatments in terms of the width and thickness of the injection layer. Then the price of the injected material (*IC*) was calculated per hectare. Then the total cost (*TC*) of the injected material plus operating costs was calculated.

Similarly, the second part of the measurements included determining the effect of adding the treated cardboard injected sub-soil layer on decreasing the permeability of the sandy soils by estimating the total water applied. First, the total water applied (consumed water) (*Wa*) was estimated by recording the irrigation level and its monthly quantity with the aid of weather station data for the experimental sites. Then, the water saved percentage (*Ws*) was calculated using Eq. 8.

$$Ws=100-(Wa_{ex.}/Wa_{co.})\times 100 \tag{8}$$

where: *Ws*: water saving percentage %, $Wa_{ex.}$: the experimental water applied, m^3 ha^{-1} and $Wa_{co.}$: the control water applied, m^3 ha^{-1}.

While the required water for the root zone (*Wr*) was measured using technical sensors installed at 0.45 m depth and every 0.1 m in layers for the crop row in-between two healthy plants. The characteristics of the neutron hygrometer are CPN, 50mCi. (hydroprobe 503 DR), with a source of americium-241 beryllium, according to the International Atomic Energy Agency (IAEA, 2008) was used. Also, the root water storage (W_{st}) was measured by the sum of the water storage for each soil level to a depth of 0.45 m. As well, the water storage efficiency ($S\eta$) was determined according to Irmak *et al*., 2011 as presented in Eq. 9.

$$S\eta=(W_{st}/W_r)\times 100 \tag{9}$$

Figure 3. The cardboard injection prototype: 1- furrow openers; 2- cardboard distributor; 3- coverage unit; 4- chassis; 5- lateral slider; 6- cardboard mixing unit; 7- operating switches; 8- hopper.

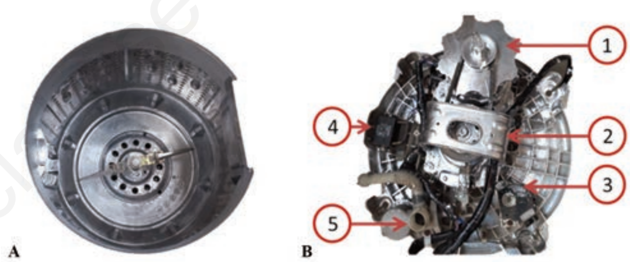

Figure 4. The cardboard mixing unit: A) upper view; B) lower view: 1- mixing AC motor; 2- gearbox; 3- tensioner motor; 4- capacitor; 5- discharge valve.

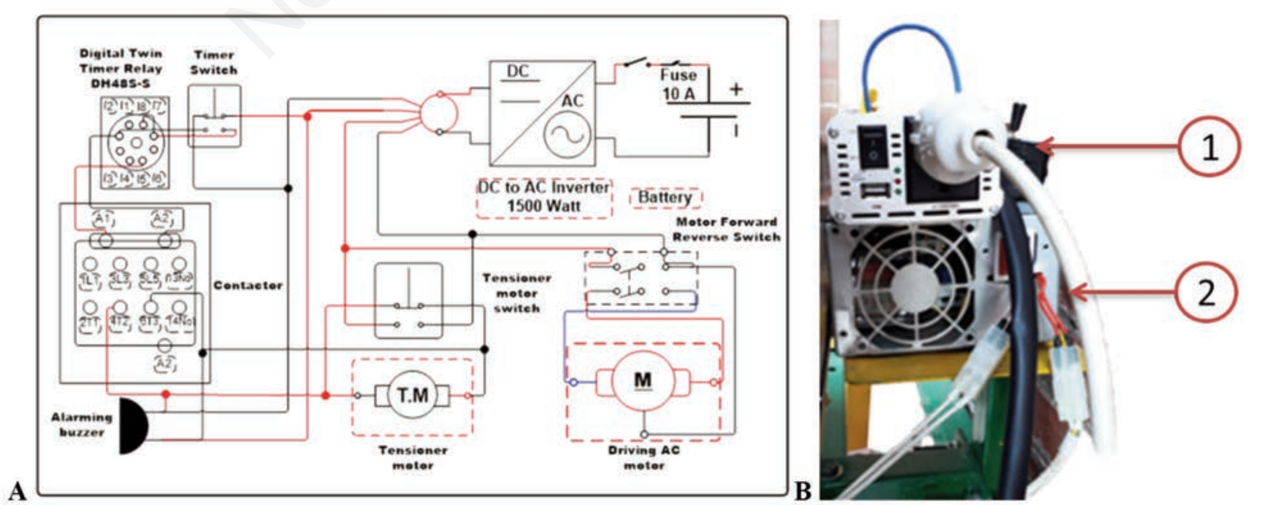

Figure 5. The electrical controlling unit: A) the electrical circuit; B) the control unit: 1- the DC-AC inverter 1500W; 2- the digital timer.

where: $S\eta$: water storage efficiency, %; W_{st}: root water storage, m^3 ha^{-1}; W_r: root water required, m^3 ha^{-1}.

As shown in Eq. 10, the soil moisture content (*Mc*) was calculated using two separate random samples collected from the tested sites to estimate the *Mc1* moisture content before irrigation and *Mc2* moisture content after irrigation at depths of 250, 350, and 450 mm using the gravimetric method according to Kodikara *et al*. (2014). Also, the irrigation rate (*In*) was recorded continuously during the growing seasons.

$$Mc = (W_1 - W_2)/W_2 \times 100 \qquad (10)$$

where: W_1: soil sample wet weight, g and W_2: soil sample dried weight after 72 h at 105°C.

The third part included growing crop measurements by determining the yield quantity (*Y*) by gathering and weighing the harvested crop at the end of the planting season. As well, determining irrigation water productivity (*Wp*) uses an Eq. 11, according to Playan and Mateos (2006).

$$Wp = Y/Wa \qquad (11)$$

where: *Wp*: irrigation water productivity, g m^{-3}; *Y*: total yield, g ha^{-1}; *Wa*: total water applied, m^3 ha^{-1}.

Soil chemical and physical properties

The collected soil samples (0-250, 250-350, and 350-450 mm) were air-dried, crushed, and sieved through a 2.0 mm sieve. The physical and chemical characteristics of the sampled soil (before and after planting) were determined using Klute (1986) and Page *et al.* (1982), respectively, and the results are shown in Appendix Tables 1 and 8.

Statistical analysis

Data were statistically analysed using the SPSS and Minitab software programs. Stepwise regression analysis and the ANOVA test were used to determine significance levels of 0.01 and 0.05 for the tested factors. In addition, the obtained results represented the mean results of the two tested seasons. The measurements were divided into three major sections: first, the injection prototype performance tests with a probability of $P<0.05$, followed by a comparison of the physical properties of sandy soils and the growing crop with a probability of $P<0.01$.

Results and discussion

The injected cardboard layer specifications

As presented in (Figures 6 and 7), the obtained results displayed directly proportional relationships between the forward speeds (*S*) and, the measured injection rate (*Ir*), and the cardboard layer thickness (*Lt*) for the tested variables. The results showed

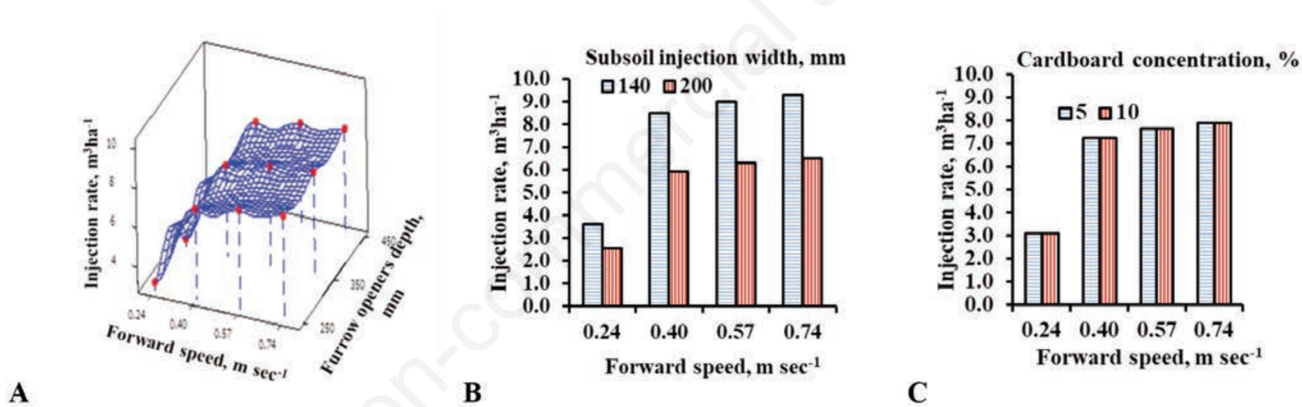

Figure 6. The effect of forward speeds on the injection rate at various: A) furrow openers depths; B) subsoil injection widths; and C) cardboard concentrations.

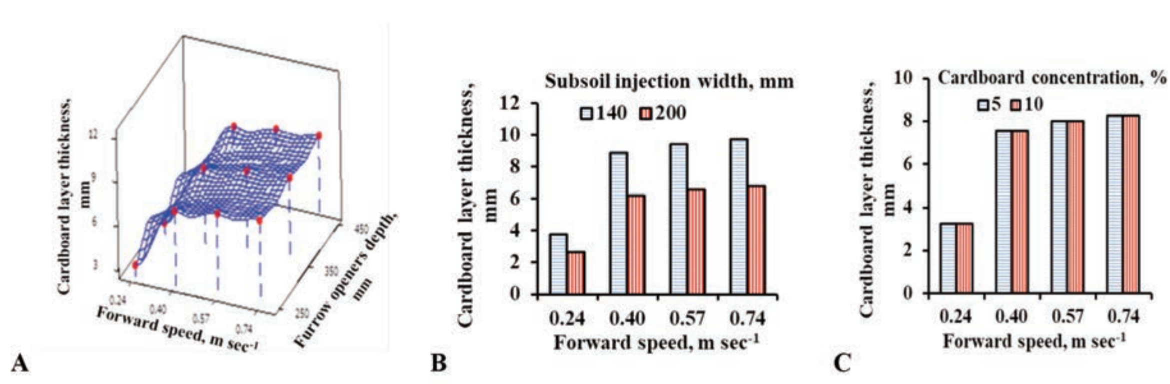

Figure 7. The effect of forward speeds on the cardboard layer thickness at various: A) furrow openers depths; B) subsoil injection widths; and C) cardboard concentrations.

that increasing the forward speed from 0.24 to 0.74 m sec^{-1} increased the amount of injected cardboard at all furrow opening depth (*D*), injection width (*W*), and cardboard concentration (*C*) variable levels. As shown in Figure 6A-C, the maximal values of the injection rate (*Ir*) were 7.92, 9.31 and 7.92 m^3 ha^{-1} respectively, for the '*D* 450 mm, *W* of 140 mm, and *C* of 10%', at the highest value of *S* of 0.74 m sec^{-1}. The minimal values for the *Ir* were 3.09, 2.54 and 3.09 m^3 ha^{-1} for the *D* of 250 mm, 200 mm of *W,* and 5% of *C* at the lowest value of (*S*) 0.24 m sec^{-1}.

Also, as shown in Figure 7A-C, the highest values of the *Lt* were 8.25, 9.70 and 8.25 mm respectively, for *D* 450 mm, *W* 140 mm, and *C* 10%, at the highest value *S* of 0.74 m sec^{-1}. The lowest values for *Lt* were 3.22, 2.65 and 3.22 mm, respectively, for *D* 250 mm, *W* 200 mm, and *C* 5% at the lowest value *S* of 0.24 m sec^{-1}. Generally, the maximum quantity of card cardboard was 9.31 m^{3}ha^{-1}, while the maximum layer thickness was 9.70 mm at 0.74 m sec^{-1} of forward speed, 450 mm of furrow openers depth, 140 mm of injection width, and 10 % of solution concentration. The obtained results are explained by the synchronised electrical methodology using the electrical controller that increases the amount of injected cardboard layer thickness while increasing the forward speeds relatively according to soil depth. Furthermore, the injection layer's thickness, depth, and width were consistent with the theoretical considerations of similar studies (Bruand *et al.,* 2004; Badr *et al*., 2012; Ayas, 2013; Hengl *et al*., 2017). The stepwise regression methodology was applied to determine the best prototype setting, as shown in the Eqs. 12 and 13.

$$(Ir),\ m^3ha^{-1} = 8.635 + 8.856\ S - 0.038\ W\ \text{(Stepwise method)} \quad (12)$$

$$(Lt),\ mm = 0.904 + 0.925\ S - 0.004\ W\ \text{(Stepwise method)} \quad (13)$$

The consumed energy

Consequently, as shown in Appendix Figure 1, the gained results followed an opposite proportional relationship between the forward speeds (*S*) and the consumed energy (*CE*) of the tested variables (*D*, *W* and *C*). Fuel consumption rates for the injection operations are listed in Appendix Table 5. As shown in Appendix Figure 1A-C and Appendix Table 5, the optimal values of the consumed energy (*CE*) (were 196.08, 193.57 and 193.06 kWh ha^{-1}) respectively, for the '*D* of 450 mm, *W* of 200 mm, and *C* of 10%', at the lowest value of *S* of 0.24 m sec^{-1}. On the other hand, the minimal values for the *CE* were (69.96, 71.85 and 72.09 kWh ha^{-1}) respectively, for the '*D* of 250 mm, *W* of 140 mm and C of 5%', at the highest value of (*S*) 0.74 m sec^{-1}.

The maximum values of the fuel consumption (*F*) were (6.47, 6.28, and 6.25 L h^{-1}) for *D* 450 mm, *W* 200 mm, and *C* 10%, respectively, at the highest value (*S*) of 0.74 m sec^{-1}, while the minimum values for *F* were (4.42, 4.54, and 4.56 L h^{-1}) for *D* 250 mm, *W* 140 mm, and *C* 5%, respectively, at the lowest value (*S*) of 0.24 m sec^{-1}. The results indicated that increasing the forward speeds from 0.24 to 0.74 m sec^{-1}, it would oppositely decrease the consumed energy at all variable levels for (*D*, *W*, and *C*). It could be explained that as forward speeds increased, so did the fuel consumption rate, and vice versa for the energy consumed with increasing both depth and width of the formed furrows during injection operations. Furthermore, the power regression analysis for the measured consumed energy (*CE*) was presented in the Eq. (14).

$$(CE)\ kWh\ ha^{-1} = 219.495 - 233.105\ S + 0.023\ D + 0.017\ W + 0.099\ C \quad (14)$$

The prototype field efficiency and capacity

Hence, the obtained results cleared direct proportional relationships between the forward speeds (*S*) and the field efficiency (*Fe*) and capacity (*Fc*) at (*D, W* and *C*) factor levels, as illustrated in Appendix Figure 2 and Appendix Table 5. Furthermore, the results were statistically significant ($P<0.05$) for the prototype field efficiency and capacity, as shown in Appendix Table 5.

As shown in Appendix Figure 2A-C, the highest values of the field capacity (*FC*) (were 0.281, 0.276 and 0.276 ha h^{-1}) respectively, for the '*D* of 450 mm, *W* of 200 mm, and *C* of 10%', at the highest value of *S* of 0.74 m sec^{-1}. Conversely, the lowest values for the *FC* were (0.074, 0.076 and 0.076 ha h^{-1}), respectively, for the '*D* of 250 mm, *W* of 140 mm and *C* of 5%', at the lowest value of (*S*) 0.24 m sec^{-1}.

The results indicated that increasing the forward speeds from 0.24 to 0.74 m sec^{-1} directly increased the field efficiency at all variable levels (*D, W*, and *C*) from 75.03 to 89.05%. The proposed results could be explained when the forward speeds increased and the consumed time decreased relatively compared to both measured field efficiency and field capacity, in agreement with the principles of farm machinery from Kepner *et al.* (1982). However, as shown in equations (15 and 16), the regression analysis for prototype field efficiency (*Fe*) and capacity (*FC*) was estimated.

$$(Fe),\ \% = 61.969 + 23.945\ S + 0.015\ D + 0.011\ W + 0.077\ C \quad (15)$$

$$(FC),\ ha\ h^{-1} = -0.036 + 0.398\ S + 0.000032\ D + 0.000025\ W\ \text{(Stepwise method)} \quad (16)$$

The draft force and specific draft

Moreover, the obtained results followed direct proportional relationships between the forward speeds (*S*) and the draft force (*dF*), and the specific draft (*Sd*), as shown in Appendix Figure 3 and Appendix Table 5. The results indicated that increasing the forward speeds from 0.24 to 0.74 m sec^{-1} could directly increase the measured draft force (*dF*) at all variable levels for (*D, W* and *C*), as listed in Appendix Table 5. As shown in Appendix Figure 3A-C, the maximum values of the specific draft (*Sd*) were 10,300, 8010 and 8010 Pa, respectively, for the '*D* of 450 mm, *W* of 200 mm and *C* of 10%', at the highest value of *S* of 0.74 m sec^{-1}. The minimum values for the *Sd* were 1750, 2440 and 2440 Pa, respectively for the '*D* of 250 mm, *W* of 140 mm and *C* of 5%', at the lowest value of (*S*) 0.0.24 m sec^{-1}.

The results indicated that increasing the forward speeds from 0.24 to 0.74 m sec^{-1} directly increased the measured draft force (*df*) at all variable levels for (*D, W*, and C) from 4440 to 8390 N. The results were explained because when forward speeds increase, the soil penetration force per unit area also increases correspondingly due to the higher penetration depth using the digger type of the furrow opener units. These results are consistent with all previous studies (Paco *et al.,* 2006; Hengel *et al.,* 2017). The regression Eqs. 17 and 18 for draft force (*dF*) and specific draft (*Sd*) were estimated.

$$(dF)\ N = -3094 + 6351\ S + 181\ D\ \text{(Stepwise method)} \quad (17)$$

$$(Sd)\ Pa = -54132 + 111031\ S + 148\ D\ \text{(Stepwise method)} \quad (18)$$

Economic evaluation

The highest values of the total injection costs (*TC*), including both the price of the used material and the operating costs for the prototype and the tractor, were 269.95, 269.84, and 265.28 USD ha^{-1} for the '*D* of 250 mm, *W* of 140 mm, and *C* of 5%', respectively, at S of 0.24 m sec^{-1}. The lowest TC values were (125.81, 116.24, and 126.96 USD ha^{-1}) for the 'D of 450 mm, W of 200 mm, and C of 10%', respectively, at the minimal value of (S) 0.74 m sec^{-1}. According to the Oida (1997) methodology, the new technique reduced the total cost *versus* the cost of silt injection from 30 to 66.51%. The cost of injection has decreased because of the low price of cardboard compared to silt. The cardboard price does not exceed a third of the price of silt and is close to it in efficiency. However, the results indicated that increasing the forward speeds from 0.24 to 0.74 m sec^{-1} could decrease the (TC) at all variable levels (D, W and C), as listed in Appendix Table 6.

The water saved percentage

The measured results represented a clear positive proportional relationship between the forward speeds (S) and the root water applied (consumed water) (Wa) to the tested variables (D, W and C), as viewed in Appendix Figure 4. As illustrated in Appendix Figure 4A-C, the highest values of the (Wa) were 6411.54, 6306.84 and 6302.52 m^3 ha^{-1}, respectively for the 'D of 450 mm, W of 200 mm and C of 10%', at an S of 0.74 m sec^{-1}. The lowest values for the (Wa) were 5298, 5393.04 and 5402.04 m^3 ha^{-1}, respectively, for the 'D of 250 mm, W of 140 mm and C of 5%', respectively at the lowest value of (S) 0.24 m sec^{-1}. However, the water saved percentages (Ws) values obtained from the proportion relation between Wa for the experimental plots (Wa) compared to the control plots and the water storage efficiency were listed in Appendix Table 7. Consequently, the obtained results were in agreement with Guswa, 2008 under similar climatic conditions. These results were obtained because of highly impregnated cardboard features made from cellulose fibres. As a result, the statistical analysis shown in Appendix Table 7, was listed with probability ($P<0.05$). In addition, a linear regression analysis was conducted for the total water applied (Wa), as presented in Eq. 19.

$$(Wa),\ m^3\ ha^{-1} = 4461.762 + 1724.064\ S + 1.066\ D + 0.808\ W + 5.538\ C \quad (19)$$

The soil moisture content and irrigation rate

As seen in Appendix Figure 5, the measured results showed direct proportional relationships between the forward speeds (S) and the soil moisture content (Mc) before ($Mc1$) and after ($Mc2$) irrigation at the tested variables D, W and C. Furthermore, as shown in Appendix Figure 5A-C, the maximal values of the $Mc1$ *and* $Mc2$ were 13.74, 13.63 and 13.62 and 17.17, 17.03 and 17.02% (control, 12%) respectively for the 'D of 450 mm, W of 200 mm and C of 10%', at the S of 0.74 m sec^{-1}. The minimal values for $Mc1$ *and* $Mc2$ were 12.87, 12.96 and 13.02 and 16.09, 16.20 and 16.28% (control, 14%), respectively, for the 'D of 250 mm, W of 140 mm, and C of 5%', at the lowest value of (S) 0.24 m sec^{-1}. During the planting seasons, the irrigation rate (In) was decreased by 12-24% *versus* the control. Also, the ANOVA analysis for the tested variable levels had a probability of $P<0.05$. As a result, regression analysis was performed on the soil moisture contents ($Mc1$ *and* $Mc2$) before and after irrigation, respectively, as shown in the Eqs. 20 and 21.

$$(Mc1),\% = 12.386 + 1.01\ S + 0.001\ D + 0.001\ W + 0.003\ C \quad (20)$$

$$(Mc2),\ \% = 15.487 + 1.263\ S + 0.001\ D + 0.001\ W + 0.003\ C \quad (21)$$

The results of the measured soil moisture content gave good evidence of the success of the used technique, which improved the soil properties by capturing the water content in the sandy soils for long periods. Although the yield increment ratios increased by using the subsoil injection cardboard layer, that improved the moisture content around the plants' roots and the soil properties, which grew the plants in healthy conditions instead of the drought conditions in the hot weather. From the gathered data, the soil moisture content had the same measured trend as in the previous study by Mazza *et al.* (2014) using an organic matter supplement. However, the conducted results for the measured soil moisture data were very close to the measured ones for the studies (Rao *et al.,* 2012; Kodikara *et al.,* 2014).

Crop yield and the irrigation water productivity

The harvested crop of potatoes ranged from 35.33 to 42.74 t ha^{-1} with an increment ratio over control (28.8 t ha^{-1}) of 18.48 to 32.62%, as listed in Appendix Table 5. Whereas the potato crop is classified as a water-consumed crop, which approaches optimal productivity levels in the cardboard-injected sandy soils due to their improved features.

The irrigation water productivity (Wp) was approximately 6670 g m^{-3}, representing the yield weight division quotient on the water applied. It means that every 1 m^3 of water produces a net weight of potato yield of around 6670 g. Therefore, the obtained results were in agreement with the reviewed studies (Paco *et al*., 2006; Bechtold and Naiman, 2006; Irmak *et al*., 2011; ElMashad and Hashad, 2013). Hence, the chemical analysis for the experimental planted sites at the beginning and the end of the planting seasons were listed in Appendix Table 8.

Conclusions

This study proposed a new cardboard-injection prototype for sandy soils. This paper determined the effect of treated cardboard utilisation on improving the sandy soil's physical properties. The tested sandy soil features were significantly improved through higher soil moisture content and lower irrigation rates. Based on the results, this technique needs deep ploughing of the soil every number of seasons, and the cost of these additional agricultural operations can equal the economic cost reduction from the rates of energy savings during irrigation as well as crop productivity. It can be concluded that the addition of cardboard led to a significant decrease in soil permeability in the root zone and an increase in moisture rates, reducing irrigation water consumption rates. Therefore, this waste material can be preferred for use as a soil additive. As an alternative to plastic, it is possible to make ready-made briquettes from treated compressed cardboard waste for agricultural use according to the width of the planting rows in the covering operations. Reusing agricultural waste, especially organic waste, can promote economic improvement and employment in developing countries. Therefore, managing waste for energy and soil improvement is critical. Cardboard waste paste can also be used in mulching and culture experiments as a suitable alternative when soil is not used. Furthermore, waste products such as cardboard can be recycled as feeders for other processes such as integrated organic farming. This allows maximum use of resources and increases the production efficiency.

References

Adugna G. 2016. A review on impact of compost on soil properties, water use and crop productivity. Acad. Res. J. Agric. Sci.

Res. 4:93-104.
Alberto M.C.R., Wassmann R., Hirano T., Miyata A., Hatano R., Kumar A., Amante M. 2011. Comparisons of energy balance and evapotranspiration between flooded and aerobic rice fields in the Philippines. Agric. Water Manag. 98:1417-30.
Algadwi M. B., Spyropoulos E., Nawaz B. A. 2021. Erosion protection by polymer additive. Proceedings of the 2nd International Conference on Civil Engineering Fundamentals and Applications (ICCEFA'21) Seoul, South Korea Virtual Conference, November 21-23, Paper No. 112, pp. 1-12.
Asamatdinov A. 2018. New water-keeping soil additives. Modern Chem. Appl. 6:1-7.
Ayas S. 2013. The effects of different regimes on potato (Solanum tuberosum L. Hermes) yield and quality characteristics under unheated greenhouse conditions. Bulgarian J. Agric. Sci. 19:87-95.
Badr M.A., El-Tohamy W.A., Zaghloul A.M. 2012. Yield and water use efficiency of potato grown under different irrigation and nitrogen levels in an arid region. Agric. Water Manag. 110:9-15.
Balba A. M. 1995. Management of problem soils in arid ecosystems. Lewis publishers. CRC Press Inc., New York, NY, USA, pp. 205-270.
Bechtold J. S., Naiman R. J. 2006. Soil texture and nitrogen mineralization potential across a riparian top sequence in a semi-arid savanna. Soil Boil. Biochem. 38: 1325-33.
Bengough A.G., Mullins C.E. 1991. Penetrometer resistance, root penetration resistance and root elongation rate in two sandy loam soils. Plant Soil 131:59-66.
Bruand A., Hartmann C. , Ratana-Anupap S., Sindhusen P., Poss R., Hardy M. 2004. Composition, fabric, and porosity of an Arenic Haplustaff of Northeast Thailand. Relation to penetration resistance. Soil Sci. Soc. of Am. J. 68:185-93.
Duncan R.R., Carrow R.N., Huck M. 2000. Understanding water quality and guidelines to management. USGA Green Section Record 38:14-24.
El-Halim A., Kumlung A. 2015. Modification of sandy soil hydrophysical environment through bagasse additive under laboratory experiment. Int. Agrophy. 29:101-6.
ElMashad M., Hashad A. S. 2013. Improving the strength of sandy silt soils by mixing with cement kiln dust. J. Eng. Sci. (JES) 41:1421-31.
Fuat L. U.L.E., Gürdil G.A.K., Balada İ., Demirel B. 2018. The effects of cardboard for enhancing water holding capacity of soil. ÇOMÜ Ziraat Fakültesi Dergisi. 6:67-71.
Guswa A.J. 2008. The influence of climate on root depth. A carbon cost-benefit analysis. Water Resour. Res. 44:1-11.
Hengl T., Jesus J. M. De., Heuvelink G.B., Gonzalez M.R, Kilibarda M., Blagotic A., Kempen B. 2017. Soil Grids 250 m. Global gridded soil information based on machine learning. PLoS One e0169748, 12:1-40.
Hunt D. 1983. Farm Power Machinery Management. 8th ed. Iowa State University, Ames, IA, USA.
Huntington T.G. 2006. Available water capacity and soil organic matter. Encyclopedia of Soil Science. 2nd ed. 1:139-43.
IAEA, 2008. Field estimation of soil water content. practical guide to methods, instrumentation and sensor technology. Training course series 30, Vienna. Available from: https://www-pub.iaea.org/MTCD/publications
Irmak S., Odhiambo L.O., Kranz W.L., Eisenhauer D. E. 2011. Irrigation efficiency and uniformity, and crop water use efficiency. Biol. Syst. Engine. Papers Publ. 451:2-8.
Kepner R.A., Bainer R., Barger E.L. 1982. Principles of farm machinery. 3rd ed. AVI pub Co. Westport, CT, USA, pp. 464-8.
Klute A. 1986. Methods of soil analysis. part 1 physical and mineralogical methods 2nd ed. The American Society of Agronomy, Inc. Soil Science Society of America, Inc. 5:635-62.
Kodikara J., Rajeev P., Chan D., Gallage C. 2014. Soil moisture monitoring at the field scale using neutron probe. Canad. Geotech. J. 51:332-45.
Ling L., Zhang Y. J., Novak A., Yang Y., Wang J. 2021. Role of biochar in improving sandy soil water retention and resilience to drought. Water 13:1-11.
Malerba M., Cerana R. 2020. Chitin-and chitosan-based derivatives in plant protection against biotic and abiotic stresses and in recovery of contaminated soil and water. Polysaccharides 1:21-30.
Manzone M. 2015. Energy consumption and CO_2 analysis of different types of chippers used in wood biomass plantations. Appl. Energy, Elsevier 156: 686-92.
Mazza C.P., Cunningham S.J., Harrison E.Z. 2014. Using organic matter in the garden. Available from: http://citeseerx.ist.psu.edu, pp. 2-12.
Nocco M.A., Smail R.A., Kucharik C.J. 2019. Observation of irrigation-induced climate change in the Midwest United States. Glob. Chang. Biol. 25:3472-84.
Nyvall J. 2002. Soil water storage capacity and available soil moisture. Water Conservation factsheet. Ministry of Agriculture. Food and Fisheries. British Colombia, Canada, pp. 1-4.
Oida A. 1997. Using personal computer for agricultural machinery management. Kyoto University. Japan. JICA publishing. Farm Machinery and Equipment, 5th ed. McGraw Hill of Publ., New York, NY, USA.
Paco T.A.D., Ferreira M.I., Conceicao N. 2006. Peach orchard evapotranspiration in a sandy soil. Comparison between eddy covariance measurements and estimates by the FAO 56 approach. Agric. Water Manag. 85:305-13.
Page A.L., Miller R.H., Keeny D.R.1982. Method of soil Analysis. Part 2. Chemical and microbiological properties 2nd ed. American Soc. of Agronomy, Inc. Soil Science Society of America, Inc. Madison, WI, USA, pp. 1159.
Playan E., Mateos L. 2006. Modernization and optimization of irrigation systems to increase water productivity. Agric. Water Manag. 80:100-16.
Rao P.K., Kumar K.S., Blessingstone T. 2012. Performance of recron-3s fibre with cement kiln dust in expansive soils. Int. J. Eng. Sci. Technol. 4:1361-6.
Sezen S.M., Yazar A., Tekin S., Eker S., Kapur B. 2011. Yield and quality response of drip-irrigated pepper under Mediterranean climatic conditions to various water regimes. Afr. J. Biotechnol. 10:1329-39.
Smith D.W., Sims B.G., O'Neill D.H. 1994. Testing and evaluation of agricultural machinery and equipment. Principles and practices. FAO. No. 110, pp.14-96.
Tutwiler R. N. 2021. Sustainable water resource management in Egypt. In Routledge Handbook on Contemporary Egypt, pp. 335-47.
Twede D., Selke S. E., Kamdem D. P., Shires. D. 2014. Cartons, crates and corrugated board. handbook of paper and wood packaging technology. DEStech Publications, Inc. pp. 500-25.
Uzoma K. C., Inoue M., Andry H., Zahoor A., Nishihara E. 2011. Influence of biochar application on sandy soil hydraulic properties and nutrient retention. J. Food Agric. Environ. 9:1137-43.